

Editing T cell repertoire by thymic epithelial cell-directed gene transfer abrogates risk of type 1 diabetes development

Fabio Russo,¹ Eliana Ruggiero,² Rosalia Curto,¹ Laura Passeri,¹ Francesca Sanvito,³ Ileana Bortolomai,¹ Anna Villa,^{1,4} Silvia Gregori,¹ and Andrea Annoni¹

¹San Raffaele Telethon Institute for Gene Therapy, IRCCS San Raffaele Scientific Institute, Via Olgettina 58, 20132 Milan, Italy; ²Experimental Hematology Unit, Division of Immunology, Transplantation and Infectious Diseases, IRCCS San Raffaele Scientific Institute, 20132 Milan, Italy; ³Pathology Unit, Division of Experimental Oncology, IRCCS San Raffaele Scientific Institute, 20132 Milan, Italy; ⁴Milan Unit, Istituto di Ricerca Genetica e Biomedica (IRGB), Consiglio Nazionale delle Ricerche (CNR), 20090 Milan, Italy

Insulin is the primary autoantigen (Ag) targeted by T cells in type 1 diabetes (T1D). Although biomarkers precisely identifying subjects at high risk of T1D are available, successful prophylaxis is still an unmet need. Leaky central tolerance to insulin may be partially ascribed to the instability of the MHC-InsB₉₋₂₃ complex, which lowers TCR avidity, thus resulting in defective negative selection of autoreactive clones and inadequate insulin-specific T regulatory cell (Treg) induction. We developed a lentiviral vector (LV)-based strategy to engineer thymic epithelial cells (TECs) to correct diabetogenic T cell repertoire. Intrathymic (it) LV injection established stable transgene expression in EpCAM⁺ TECs, by virtue of transduction of TEC precursors. it-LV-driven presentation of the immunodominant portion of ovalbumin allowed persistent and complete negative selection of responsive T cells in OT-II chimeric mice. We successfully applied this strategy to correct the diabetogenic repertoire of young non-obese diabetic mice, imposing the presentation by TECs of the stronger agonist InsulinB₉₋₂₃R22E and partially depleting the existing T cell compartment. We further circumscribed LV-driven presentation of InsulinB₉₋₂₃R22E by micro-RNA regulation to CD45⁻ TECs without loss of efficacy in protection from diabetes, associated with expanded insulin-specific Tregs. Overall, our gene transfer-based prophylaxis fine-tuned the central tolerance processes of negative selection and Treg induction, correcting an autoimmune prone T cell repertoire.

INTRODUCTION

Type 1 diabetes (T1D) is a chronic autoimmune disease mediated by T cells that infiltrate and destroy insulin-producing β cells within the pancreatic islets, often starting in childhood or adolescence.¹ The incidence of T1D has increased significantly in recent decades, particularly in young children.² Seroconversion to a detectable titer of more than one autoantibody (autoAb) specific for islet-associated antigens (Ags: insulin, Ins; glutamic acid decarboxylase 65-kDa isoform, GAD65; insulinoma-associated-2, IA-2; zinc transporter 8,

ZnT8) characterizes the pre-symptomatic stage of T1D, which in most cases evolves into overt autoimmune diabetes within a decade. Although multiple islet autoAbs are biomarkers of high-risk T1D development, the disease cannot currently be prevented. Thus, an effective prophylactic intervention remains an urgent unmet medical need.

Autoimmune responses to insulin are associated with T1D development, especially in younger patients harboring HLA DR4-DQ8. In this patient population insulin may be the initial autoantigen. The disease observed in non-obese diabetic (NOD) mice is also driven by autoimmunity to insulin. Therefore, insulin is the ideal target for testing Ag-specific tolerogenic approaches for disease prevention in NOD mice, which may have translational relevance for a subset of individuals.³⁻⁸

Human and rodent thymi are fully active in shaping the T cell repertoire only for a limited time window before undergoing an irreversible involution. Thymic epithelial cells (TECs) play a pivotal role in thymocyte selection by presenting *self*-Ag-derived epitopes. The rate of autoimmune regulator (AIRE)-driven transcription of proinsulin in medullary (m)TECs is genetically determined⁹ and impacts susceptibility to T1D, affecting thymic selection of the T cell repertoire. Thus, a weak expression of proinsulin by mTECs is associated with suboptimal negative selection of insulin-reactive T cell clones. Several strategies for Ag-specific tolerance induction have been tested to achieve Ag expression in the thymus and drive negative selection of Ag-reactive thymocytes and/or induction of regulatory T cells (Tregs).^{10,11} However, none of them employed a selective cell-targeting approach to impose the presentation of a specific epitope only by

Received 28 February 2022; accepted 29 April 2022;
<https://doi.org/10.1016/j.omtm.2022.04.017>

Correspondence: Andrea Annoni, PhD, San Raffaele Telethon Institute for Gene Therapy, IRCCS San Raffaele Scientific Institute, Via Olgettina 58, 20132 Milan, Italy.

E-mail: annoni.andrea@hsr.it

TECs, failing to fulfill safety requirements. In addition, none of them showed the capacity to achieve a profound and stable negative selection of Ag-reactive clones and drive the selection of additional Treg clonotypes to correct an autoimmune prone T cell repertoire.

We designed a lentiviral vector (LV) platform capable of establishing presentation of specific Ags in a renewable population of TECs to correct thymic selection in a model resembling young subjects at risk for T1D development. We used NOD female mice at age 5 weeks as a model of young subjects at high risk for T1D development. At this age, mice have a mature T cell compartment comprising diabetogenic T cells, and primitive InsB₉₋₂₃ responses have already started, while the β cell mass is still intact.^{12,13}

Here, we show that intrathymic (it) administration of an LV encoding for invariant-chain (Ii) fused to a portion of the Ag of interest, including immunodominant T cell epitope, represents a successful strategy to generate a stable subset of engineered TECs, by transducing the common EpCAM⁺CD49F⁺Sca-1⁺ TEC precursor.¹⁴ This results in persistent and robust presentation of autoAgs by TECs to developing thymocytes. In addition, micro-RNA142-negative post transcriptional regulation of Ii.Ag expression was exploited to target LV-driven epitope presentation to TECs. Upon transduction, TECs are permissive for transgene expression since they do not belong to a hematopoietic lineage and do not express micro-RNA142.¹⁵ By enabling presentation of the strong agonistic variant of insulin InsB9-23 carrying R22E modification, the LV platform optimizes the selection of insulin-reactive clones,¹⁶⁻¹⁸ reshaping the T cell repertoire and preventing T1D development.

RESULTS

LV-mediated transduction of the TEC progenitors enables stable transgene expression in cortical and medullary TECs

Aiming to perturb the T cell selection process, we tested whether the injection of LV into the thymus could result in a durable genetic modification of TECs. To determine distribution of transgene expression in the body and success rate of the injection procedure, NOD mice (n = 10) were intrathymically injected with luciferase-encoding LV under the control of phosphoglycerate kinase (PGK) promoter (LV.Luc, 2×10^7 transfection unit [TU]/mouse). Ten days post injection, 90% of LV-treated mice displayed a thymus-localized luciferase activity (Figure S1). To determine whether TECs can be transduced via it-LV administration, 5-week-old C57Bl6 mice (n = 6) were intrathymically injected with a GFP-encoding vector (LV.GFP, 2×10^7 TU/mouse). At 1 and 9 weeks (n = 3/time point) post LV.GFP treatment, thymi were harvested and CD45⁻ TEC-enriched cells were isolated to determine the percentage of GFP expressing TECs (EpCAM⁺), including cortical (c) (CD80^{low/int} Ly51⁺) and medullary (m)TECs (CD80⁺Ly51^{low/int}), and their common precursors (CD49F⁺Sca-1⁺) (Figure 1A). Results indicate that an average of 2.8% of TECs (CD45⁻ EpCAM⁺) expressed GFP at 1 week post treatment. The expression was stably maintained up to 9 weeks post it-LV by virtue of the transduction of 1.4% of TEC precursors (Figures 1B

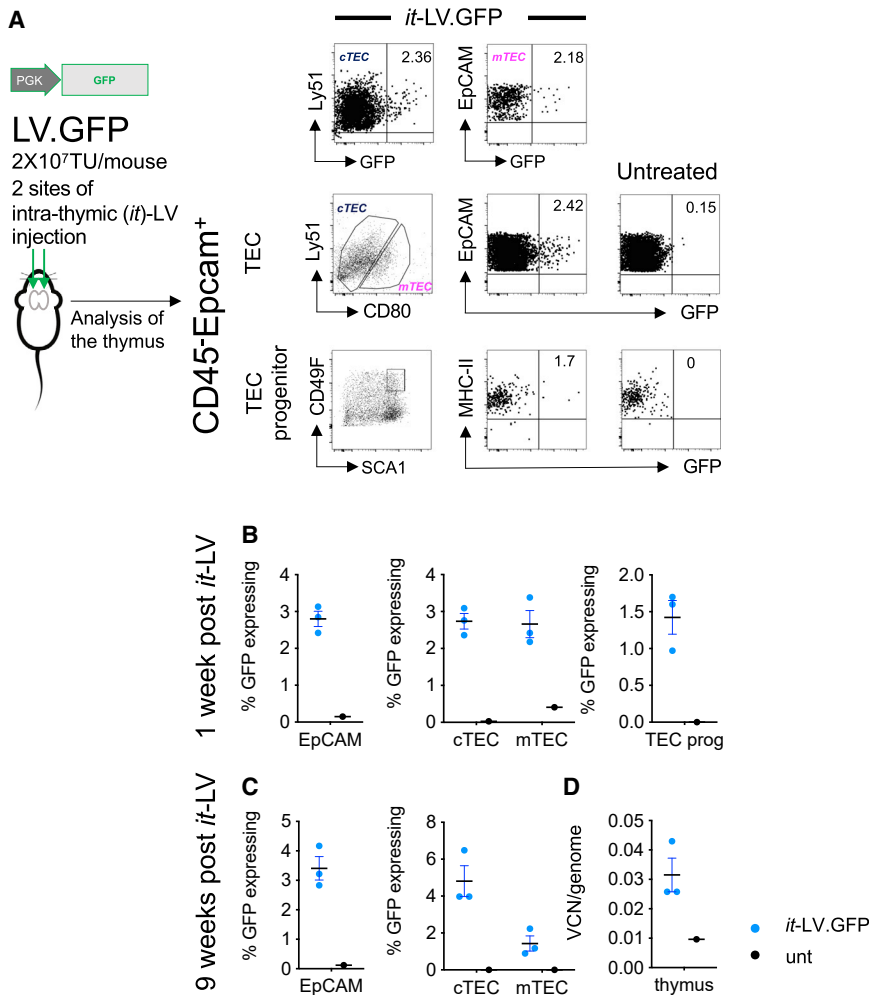
and 1C). A comparable fraction of GFP⁺ was observed in cTECs and mTECs at 1 week post it-LV (Figure 1B). Conversely, at 9 weeks post injection GFP expression was higher in cTECs, possibly due to progressive tissue disorganization (Figure 1C). Therefore, a single it-LV treatment leads to vector integration into TEC precursors, resulting in a stable modification of mature TEC compartment (Figure 1D), which persists beyond their 2-week turn-over time.¹⁹ This opens the possibility of expressing genes to modulate thymocyte selection for the entire window of activity of the primary lymphoid organ.

TEC-mediated Ag presentation imposed by it-LV gene transfer alters thymocytes selection overtime

To prove the potential of it-LV gene transfer in redirecting thymocyte selection, CD45.1 C57B16 mice (n = 9) were lethally irradiated, while lead-shielding the thymus to preserve tissue architecture and function; and bone marrow cell transplantation (BMT) from CD45.2.OT-II T cell receptor (TCR) transgenic mice was performed to achieve mixed chimerism (Figures 2A–2C). This model ensured the migration of CD45.2.OT-II T cell precursors with a known Ag-specificity for Ovalbumin₃₂₃₋₃₃₉ (OVA₃₂₃₋₃₃₉) from bone marrow (BM) to the thymus, where immature T cells will complete maturation and undergo thymic selection. As soon as CD45.2.OT-II CD4⁺ T cells were detectable in the peripheral blood of transplanted mice (week 5 post BMT), they received it-LV encoding for invariant-chain (Ii) fused to chicken Ovalbumin₃₁₅₋₃₅₃ (Ii.OVA₃₁₅₋₃₅₃) fragment (it-LV.OVA, n = 6), to achieve OVA₃₂₃₋₃₃₉ presentation by TECs, or it-LV encoding for Ii fused to GAD65₅₀₀₋₅₈₅ (it-LV.GAD65, n = 3), as unrelated Ag control. The frequency of CD45.2.OT-II CD4⁺ T cells was determined by cytofluorimetric analysis of circulating cells and the ratio [CD45.2.OT-II CD4⁺ T cells/CD45.2 CD11b⁺GR1⁺ myeloid cells] was determined at the indicated time points (Figures 2B–2D). Results showed that it-LV.OVA led to TEC transduction and consequent OVA₃₂₃₋₃₃₉ presentation in the context of major histocompatibility complex class II (MHC class II) to developing thymocytes, as confirmed by the complete negative selection of CD45.2.OT-II CD4⁺ T cells in it-LV.OVA mice. Conversely, CD45.2.OT-II CD4⁺ T cells egressed from the thymus in it-LV.GAD65-treated control mice. Of note, 2×10^7 TU/mouse dose resulted in ~3% of transgene-expressing TECs (Figure 1B); thus, in chimeric mice we expect that a similar percentage of TECs were presenting cognate Ag (OVA₃₂₃₋₃₃₉) to OT-II T cells. Since levels of engraftment mirror the composition of T cell precursors, we can estimate that up to 35% of them, originating from OT-II hematopoietic stem and progenitor cells, were negatively selected by a few LV-engineered TECs, demonstrating the potency and precision of this strategy.

Intrathymic LV gene transfer alters thymocyte selection and abrogates T1D development in NOD mice

To evaluate whether perturbing the selection of thymocytes responsive to insulin immunodominant epitope (InsB₉₋₂₃) may reduce T1D development, 5-week-old NOD female mice (n = 15) received it-LV encoding for Ii.Insulin B chain₄₋₂₉R22E (it-LV.InsB.R22E,



n = 8) or Ii.OVA₃₁₅₋₃₅₃ (*it*-LV.OVA, n = 7) as control (Figure 3A). R22E aminoacidic substitution improves stability of [InsB₉₋₂₃-IAg⁷] complex (IAg⁷ is MHC class II in NOD mice). To reduce the frequency of autoreactive diabetogenic cells already in circulation at the time of treatment, and to allow the reconstitution of the T cell repertoire conditioned by *it*-LV-driven insulin epitope presentation, the day after *it*-LV injection mice were treated with an Ab cocktail to deplete CD4⁺ and CD8⁺ T cells (Δ T) *in vivo*. After 5 weeks, the T cell compartment was almost completely reconstituted by T cells selected by the *it*-LV-conditioned thymus and by homeostatic expansion of T cells spared by the depletion regimen (Figure 3B). LV-mediated genetic modification was comparable in the two groups of *it*-LV-treated mice, as indicated by quantification of vector copy number (VCN) in the thymus (Figure 3C). Blood glucose levels (bgl) were monitored up to age 33 weeks in *it*-LV-treated mice. Results indicate that InsB₉₋₂₃R22E presentation in the context of I-Ag⁷ MHC class II molecules by TECs was able to inhibit development of T1D (Figures 3D and 3E). Infiltration of the pancreatic islets was evaluated in *it*-LV.InsB.R22E-treated mice and compared with that

Figure 1. Intrathymic LV injection leads to TEC precursor transduction ensuring persistent transgene expression by TECs

C57Bl6 mice (5 weeks old, n = 6) were injected in the thymus with LV.PGK.GFP (*it*-LV.GFP, 2 × 10⁷ TU) or left untreated as control (n = 2). (A–C) Thymus was harvested and cytofluorimetric analysis (A) was performed at 1 and 9 weeks post LV administration (B and C). Thymic CD45⁺ cells were removed by magnetic sorting and GFP expression was evaluated in the stromal compartment: TECs (CD45⁺EpCAM⁺) discriminating between cTECs and mTECs by the expression of CD80 and Ly51 markers, respectively, and TEC progenitors, defined as CD45⁺EpCAM⁺CD49F⁺Sca-1⁺. (D) Integrated vector copy number/diploid genome in the thymus were quantified by ddPCR. Single values, mean ± SEM are reported.

of diabetic NOD (bgl 350–500 mg/dL) or to normoglycemic NOD mice of age 10 and 5 weeks. Results show that insulinitis in *it*-LV-treated mice was compatible with that of normoglycemic NOD mice (Figure S2). Percentages of CD4⁺ T cells, CD8⁺ T cells, and Foxp3⁺ Tregs were determined in the pancreatic lymph nodes (PLNs) and spleen, revealing a tendency to a lymphocyte reduction in *it*-LV.InsB.R22E-treated mice (Figures S3A and S3B). Notably, there were significantly more Foxp3⁺ Tregs in the islets of *it*-LV.InsB.R22E-treated mice than in the islets of diabetic NOD mice (Figures S3C–S3E).

Histological analysis of the thymi did not show differences between *it*-LV-treated mice and untreated controls. The architecture of the thymic tissue at age ~6 months showed a typical slight decrease of the cortical layer²⁰ (Figure S4).

Based on these results, we postulate that T1D protection is due to improved processes of central tolerance to insulin by optimized induction of insulin-specific Tregs and/or negative selection of insulin-reactive T cell clones. This alteration in thymic output modulated T cell responses against insulin presented by antigen-presenting cells (APCs) in secondary lymphoid organs, overall preserving β cell mass and glucose homeostasis.

TEC-specific LV.142T gene transfer enables editing of T cell selection in the thymus

To limit off-target transgene expression in hematopoietic cells following *it*-LV administration, without the loss of TEC transduction, negative regulation mediated by hematopoietic-specific micro-RNAs was exploited. To determine whether TECs can be transduced by administering *it*-LV comprising four repeated target sequences for

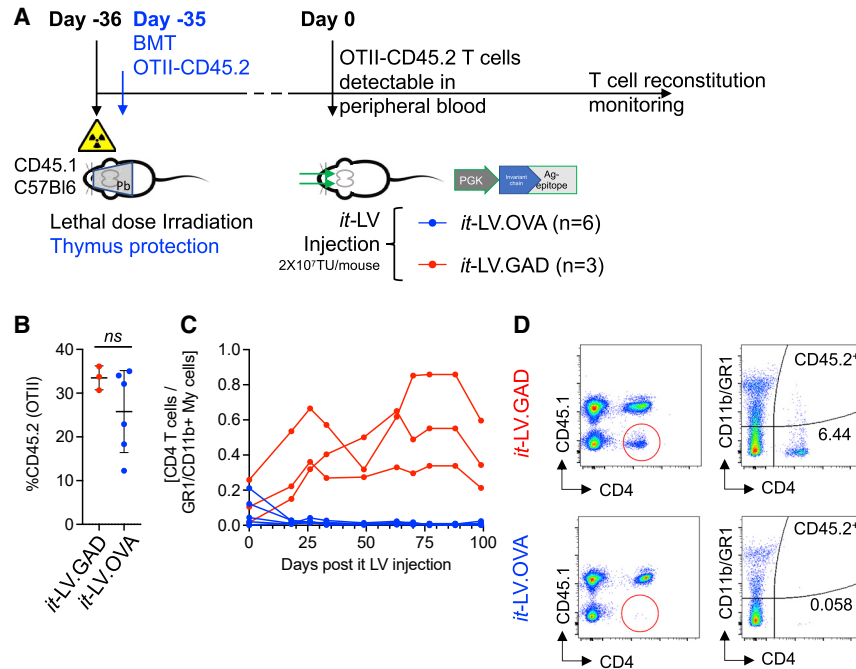


Figure 2. LV-driven presentation of an immunodominant T cell epitope by TECs results in profound and durable negative selection of Ag-reactive T cell clones

(A–D) CD45.1-C57BL6 mice (n = 9) were conditioned by lethal irradiation, protecting the thymus using a lead shield, and transplanted with CD45.2.OT-II bone marrow cells. Five weeks post BMT CD45.2.OT-II CD4⁺ T cells became detectable in circulation. Chimeric mice were treated intrathymically (it) with LV.PGK.li.OVA₃₁₅₋₃₅₃ (it-LV.OVA, n = 6) or LV.PGK.li.GAD₆₅₀₀₋₅₈₅ (it-LV.GAD, n = 3) as control. Post transplant, T cell compartment reconstitution was monitored for ~100 days after it-LV treatment (A), determining the frequency of CD4⁺ T cells and CD11b⁺GR1⁺ myeloid cells within CD45.1⁻ and OT-II-derived CD45.2⁺ cells (B). Ratio between [%CD4⁺:%CD11b⁺GR1⁺] was determined over time within CD45.2⁺ cells to normalize differences in engraftment (C). Single values, mean \pm SEM are reported. Representative dot plots of the study are reported (D).

hematopoietic-specific micro-RNA142 at 3' untranslated region, 5-week-old C57Bl6 mice received intrathymically micro-RNA regulated GFP-encoding vector (it-LV.GFP.142T, 2×10^7 TU/mouse, n = 4). One week post it-LV.GFP.142T treatment, thymi were harvested and CD45⁻ TEC-enriched cells were isolated to determine the percentage of GFP-expressing TECs (EpCAM⁺), including cTECs, mTECs, and their common precursors. Results indicate that an average of 3.6% of CD45⁻ EpCAM⁺ cells express GFP, equally represented in cTECs and mTECs, and ~1.5% of TEC precursors were GFP⁺ (Figures 4A and 4B). Therefore, it.LV.142T targeted TECs at levels comparable with those achieved by it.LV. Moreover, comparative studies confirmed that it.LV.142T targeted TECs and showed a significant reduction of transgene expression in hematopoietic cells, such as thymic and peripheral APC subsets (Figures 4C, 4D, and S5) and thymocytes (Figure S5). Thus, it.LV.142T provides a safer pattern of transgene expression, excluding cell subsets potentially able to trigger an autoimmune reaction upon presentation of a relevant autoAg in secondary lymphoid organs.

TEC-mediated InsB₉₋₂₃R22E overpresentation is effective in reshaping the T cell repertoire to achieve prevention of T1D development

To further confirm that targeting LV-driven Ag presentation to TECs represents a strategy to prevent the risk of autoimmunity, 5-week-old female NOD mice (n = 48) received intrathymic micro-RNA142-regulated LV encoding for Ii.B₄₋₂₉R22E (it-LV.InsB.R22E.142T, n = 19), with Ii.OVA₃₁₅₋₃₅₃ (it-LV.OVA, n = 8) as unrelated control Ag. To elucidate the contribution of a T cell-depleting regimen, a fraction of it-LV.142T-treated mice, as well as untreated controls, received an Abs cocktail to deplete *in vivo* CD4⁺ and CD8⁺ T cells

(Δ T) at day +1 (Figure 5A). Results indicate that the T cell-depleting regimen did not reduce the risk of T1D development *per se*, resulting in only minimally delaying disease onset. Conversely, a depleting regimen was required to achieve complete protection from T1D development in mice treated with it-LV.InsB.R22E.142T (Figures 5B and S7). LV-driven presentation of wt.InsB₉₋₂₃ did not protect from T1D development, even in association with the T cell-depleting regimen (Δ T) (Figures S6 and S7). The absence of any protection from T1D development by it-LV.OVA further demonstrates the precision of the Ag-specific activity of this strategy (Figures 5B, S6, and S7).

At the end of the observation period, frequencies of insulin-specific T cells were investigated using IAg⁷-InsB₉₋₂₃R22E tetramers. Although the frequency of insulin-specific conventional T cells (Tconv) was not altered by any treatment (Figures 5C and 5D), insulin-specific Tregs (IAg⁷-InsB₉₋₂₃R22E tetramer⁺CD25⁺CD127^{low/-}) in the spleen of it-LV.InsB.R22E.142T+ Δ T-treated mice were expanded compared with controls (Figures 5C and 5E). To elucidate whether the expansion of insulin-specific Tregs was due to newly generated clonotypes induced by it-LV.InsB₉₋₂₃R22E.142T treatment, TCR α and β sequencing was performed. Fluorescent-activated cell sorter (FACS)-purified CD4⁺ Treg-enriched population (CD25⁺CD127^{low/-}), CD4⁺ Tconv, and CD8⁺ T cells from PLN and pancreas-infiltrating T cells were isolated and analyzed (Figure S8A) from it-LV-treated mice and untreated controls. CD4⁺IAg⁷-InsB₉₋₂₃R22E-tetramer⁺ and CD8⁺H-2K^d-InsB₁₅₋₂₃-tetramer⁺ were also sorted from NOD untreated mice and sequenced to serve as reference for insulin-specific clones selected by untreated thymus (Figure S8A). We focused the analysis on TCR α , which has proven to be highly relevant for IAg⁷-InsB₉₋₂₃ recognition.²¹ In the

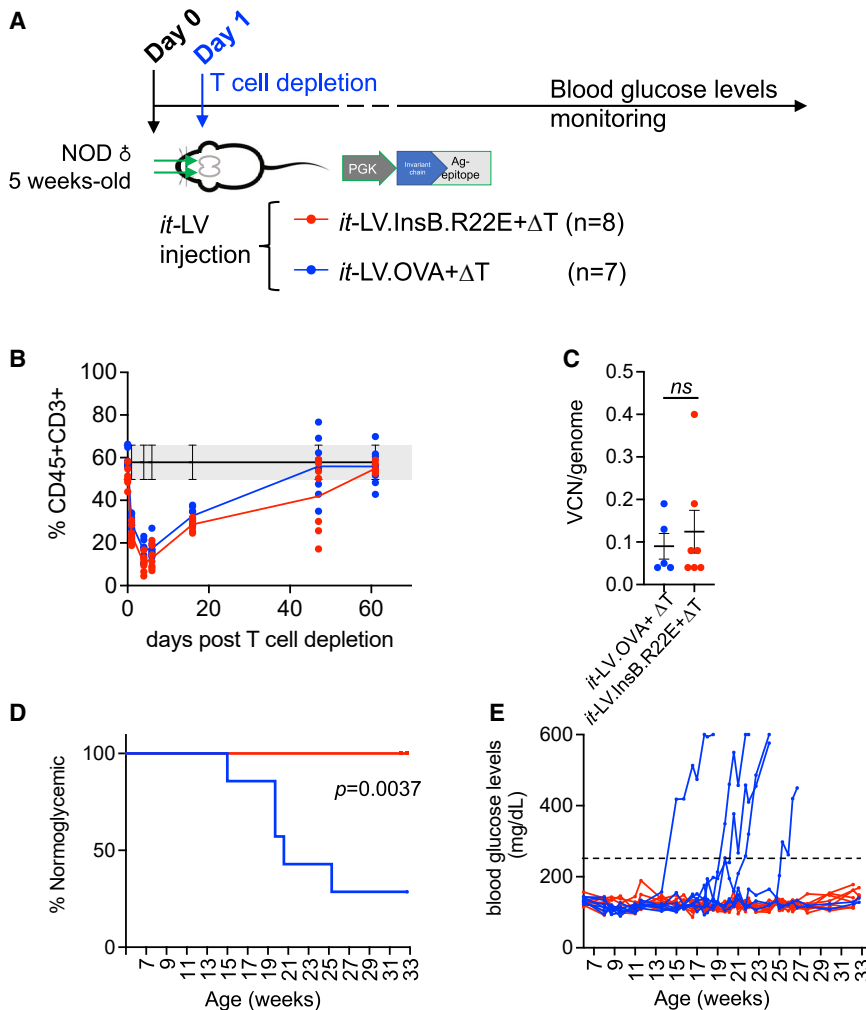


Figure 3. LV-driven presentation of InsB₉₋₂₃R22E by TECs allows suppression of T cell-mediated autoimmunity in NOD mice

(A) Five-week-old NOD female mice (n = 15) were intrathymically (it) treated with LV.PGK.li.InsB₄₋₂₉.R22E (*it*-LV.InsB.R22E, n = 8) or LV.PGK.li.OVA₃₁₅₋₃₅₃ (*it*-LV.OVA, n = 7), as control. (B) The day after, mice received intravenous anti-CD4 and anti-CD8 depleting Abs to remove at least a fraction of CD45⁺CD3⁺ mature T cells from the periphery. (C) LV conditioning of the thymus was evaluated determining integrated VCN/genome from thymic biopsy at the end of the experiment. Single values, mean ± SEM are reported (D and E) The incidence of T1D after *it*-LV therapy was evaluated by monitoring glycemia over time, considering blood glucose levels (bgl) > 250 mg/dL as the symptomatic threshold (log rank Mantel-Cox test).

In mice regardless of T cell depletion, we also found different localization of insulin-specific CD4⁺ Tconv and CD8⁺ T cells, selected for identity with TCR α CDR3 of tetramer⁺ controls from untreated animals (Figures S8A, S8F, S8H, and S8J). In protected mice (*it*-LV.InsB.R22E.142T+ΔT), we found a prevalence of insulin-specific effector clonotypes in PLNs rather than in the target organ, while in mice achieving partial protection (*it*-LV.InsB.R22E.142T) Ins-specific T effector cells were detected within the pancreas. Therefore, *it*-LV.InsB.R22E-associated bona fide Treg clones co-existed with effector cells in the PLNs of protected mice, while they were within the target organ in mice with incomplete protection (Figures 6G and 6H). Overall, these results suggest that *it*-LV-driven Tregs regulated insulin-specific T cell responses in PLNs of *it*-LV.InsB.R22E.142T+ΔT-treated NOD mice, thus inhibiting progressive erosion of the β cell mass.

PLN Tregs of *it*-LV.InsB.R22E.142T+ΔT mice, which are protected from T1D, we found sharing of several clonotypes (Figure 6A) and, among the 23 TCR α complementarity-determining region 3 (CDR3) Treg sequences shared, 17 were found exclusively in mice treated with *it*-LV.InsB.R22E.142T, with or without T cell depletion (Figure 6B, in yellow). Among the 17 *it*-LV.InsB.R22E.142T treatment-associated clones, only 6 were ascribable to the Treg compartment (Figure 6C, in red) since they were not shared with PLN Tconv sequences. One clonotype was shared by CD4⁺ Tconv from untreated NOD mice, suggesting that *it*-LV treatment possibly promoted its conversion into Tregs. Interestingly, five of the seven latter clonotypes were also found in pancreas-infiltrating T cells of *it*-LV.InsB.R22E.142T-treated mice, but not in *it*-LV.InsB.R22E.142T+ΔT mice (Figure 6D, in white), suggesting a different Treg dynamic and localization within the two groups. Therefore, these seven CDR3 sequences were regarded as bona fide Treg clonotypes induced by *it*-LV.InsB.R22E.142T treatment, either in PLNs (in mice receiving T cell depletion and achieving full protection) or in pancreatic infiltrates (in the absence of T cell depletion and with only partial protection from T1D) (Figures 6E and 6F).

lated insulin-specific T cell responses in PLNs of *it*-LV.InsB.R22E.142T+ΔT-treated NOD mice, thus inhibiting progressive erosion of the β cell mass.

In conclusion, these data demonstrate that selective targeting presentation of hyper-agonist T cell epitopes to TECs in combination with a T cell-depleting regimen is an effective preventive strategy to dampen the diabetogenic potential of T cell repertoire, resulting in protection from autoimmune T1D.

DISCUSSION

This study shows that the T cell repertoire that predisposes NOD mice to autoimmune T1D can be modified by the intrathymic administration of LV for TEC-directed gene transfer to achieve central tolerance to insulin and preventing autoimmunity. The concept of modulation of Ag-specific central tolerance has been explored in the past in different models of autoimmune diseases by vector-mediated expression or direct injection of the protein of interest into the thymus.^{11,22} We have substantially improved several aspects of this

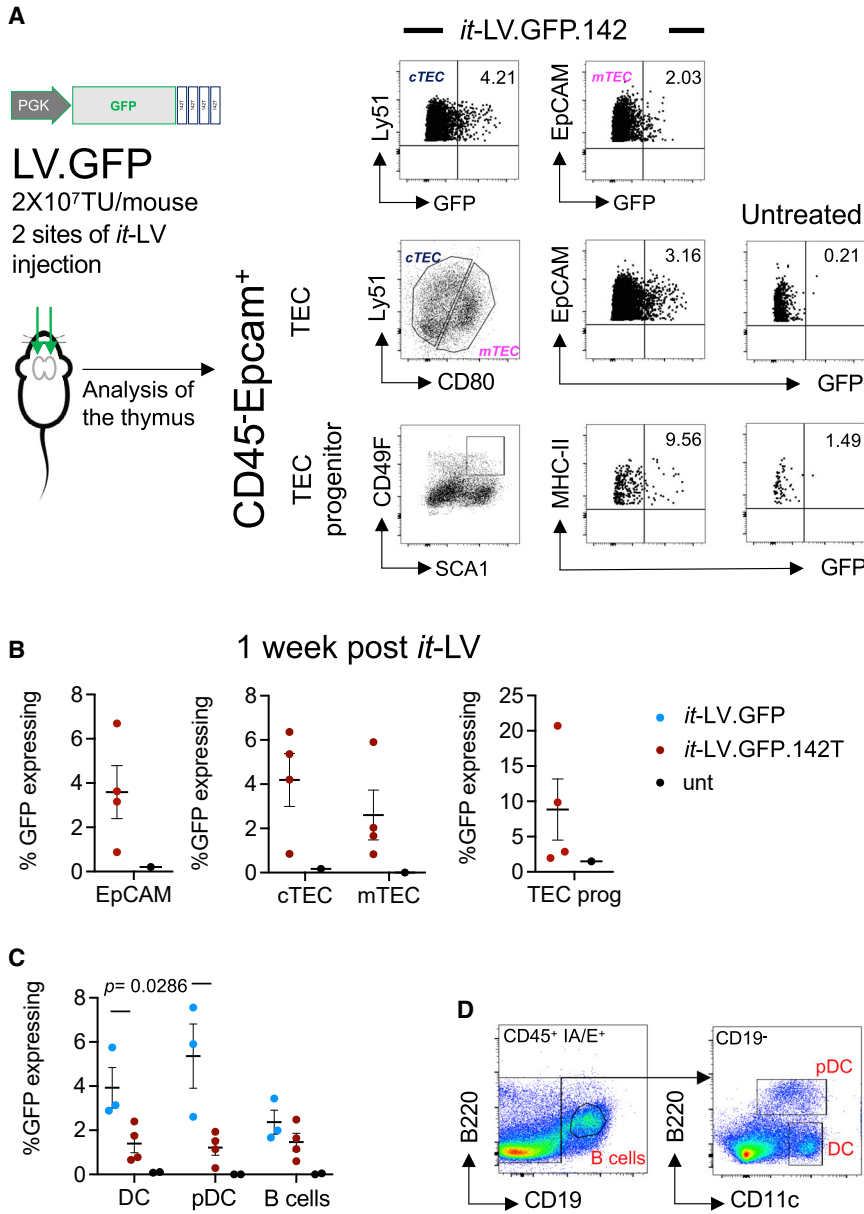


Figure 4. Intrathymic injection of LV, including micro-RNA142 regulatory elements allowed a more precise targeting of transgene expression in TECs

C57Bl/6 mice (5 weeks old, $n = 14$) were injected in the thymus with LV.PGK.GFP.142T (*it*-LV.GFP.142T, $n = 8$, 2×10^7 TU), *it*-LV.PGK.GFP (*it*-LV.GFP, $n = 3$, 2×10^7 TU) or left untreated as control ($n = 3$). (A) Thymus was harvested and cytofluorimetric analysis was performed at 1 week post LV administration. (B) Thymic CD45⁺ cells were removed by magnetic sorting and GFP expression was evaluated in the stromal compartment: TECs (CD45⁺EpCAM⁺), discriminating between cTECs and mTECs by the expression of CD80 and Ly51 markers, and TEC progenitors, defined as CD45⁺EpCAM⁺, CD49F⁺, Sca-1⁺. (C) To evaluate micro-RNA142 negative post transcriptional regulation in thymic CD45⁺, GFP expression was compared in antigen-presenting cells. DC, dendritic cell; pDC plasmacytoid-DC and B cells. (D) Single values, mean \pm SEM are reported (Mann-Whitney test). Representative dot plots of the analysis are reported.

strategy, defining a specific and efficacious platform, potentially applicable to subjects at risk of T1D. We show that a single LV dose is sufficient to engineer less than 5% of TEC that, despite low frequency, successfully promotes negative selection of highly represented clones (e.g., TCR transgenic OT-II thymocytes) and achieves an almost complete protection from T1D development in NOD mice, predominantly through the selection of a new family of thymic-derived Tregs. Previous attempts based on transgenic LV-mediated expression of proinsulin have shown only a partial prevention of T1D in NOD mice,²² and their potential for clinical translation remains elusive. Bettini and colleagues elegantly showed that forced presentation of wt-InsB immunodominant epitope by professional APCs in the

thymus of specific retro-genic mice promoted induction of Ag-specific Tregs, while presentation of the modified epitope (InsB₉₋₂₃R22E) led to negative selection of a specific insulin-reactive T clone.²³ Although the use of retro-genic mice represents a precise approach to study mechanisms of thymic selection, results were limited to a few insulin-specific clones, losing the complexity that results from the selection of multiple clones potentially reactive to the *it*-LV-encoded epitope. We show that InsB₉₋₂₃R22E presentation is able to promote expansion of insulin-specific Tregs in fully immunocompetent NOD mice. Unfortunately, in our experimental settings we were unable to definitely define whether negative selection of InsB₉₋₂₃-specific clones occurred. However, altering the strength of TCR signaling of InsB₉₋₂₃ by introducing R22E aminoacidic substitution we are likely altering the fate of several clonotypes; therefore, correcting the T cell repertoire of naive T cells and Tregs. We can envisage that, among billions of clonotypes, those recognizing InsB₉₋₂₃, destined to be naive T cells in untreated NOD, will be selected to be Tregs, or deleted after encountering InsB₉₋₂₃R22E-presenting mTECs.

Alterations of central tolerance mechanisms in autoimmunity are still not completely understood. The immunodominant autoAg InsB₉₋₂₃, while restricted to T1D-predisposing MHC class II IAg⁷ molecule in NOD mice, as well as the homologous HLA-DQ8 in humans, generates an unstable MHC-peptide complex,¹⁷ which seems to lower TCR T cell avidity, leading to inadequate T cell selection.²⁴ To optimize

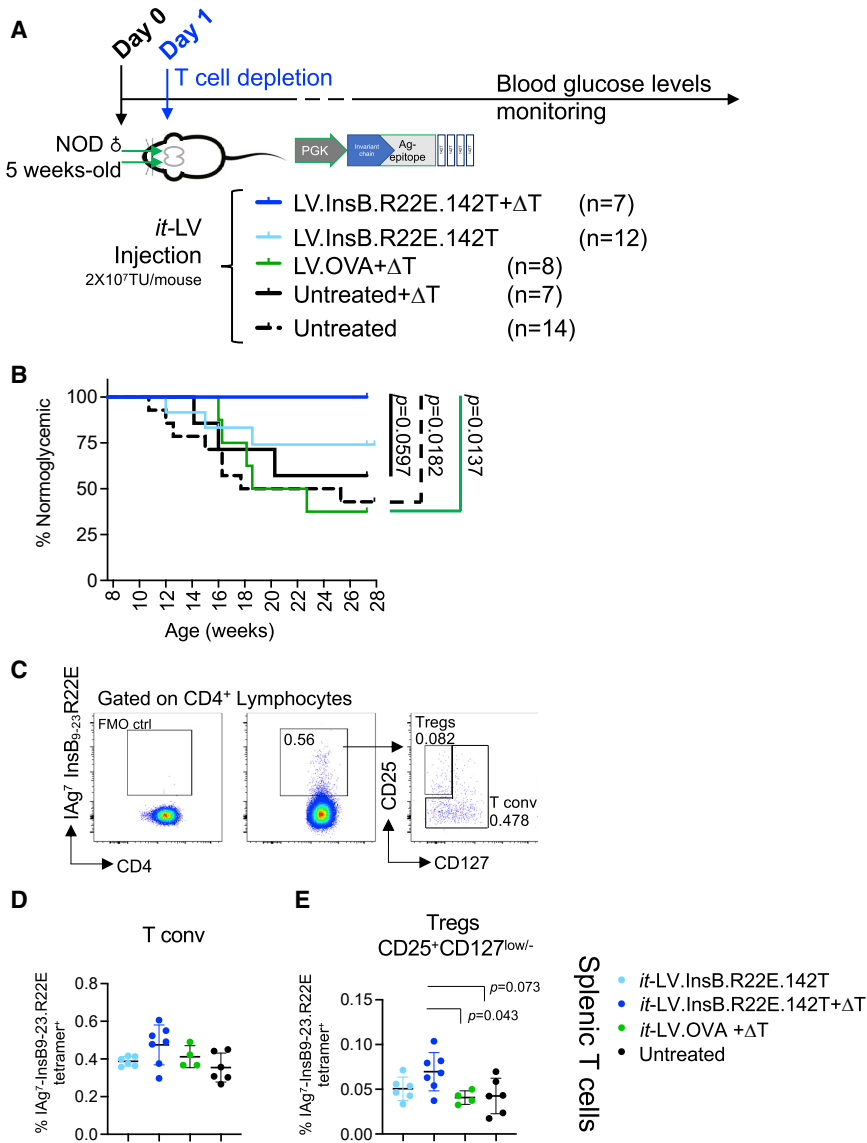


Figure 5. Intrathymic injection of LV encoding for li.InsB₄₋₂₉R22E followed by T cell depletion resulted in protection from autoimmune T1D

(A) Five-week-old NOD female mice (n = 48) were intrathymically treated with LV.li.InsB₄₋₂₉R22E.142T \pm T cell depletion (it-LV.InsB.R22E.142T+ Δ T, n = 7; it-LV.InsB.R22E.142T, n = 12), LV.PGK.li.OVA₃₁₅₋₃₅₃ + T cell depletion (it-LV.OVA+ Δ T, n = 8), or left untreated \pm T cell depletion, as control (n = 7, n = 14). (B) Glycemia was monitored from age week 10 to 28 and incidence of T1D is reported. Mice were considered normoglycemic with bgl < 250 mg/dL (log rank Mantel-Cox test). (C–E) At the end of the observation, percentages of InsB₉₋₂₃-specific CD4⁺ T conv and Treg (CD25⁺CD127^{low/-}) cells were determined in the spleen by IAg⁷ tetramer immunophenotype. Single values, mean \pm SEM (%) within CD4⁺ T cell population and representative dot plots are reported (Mann-Whitney test).

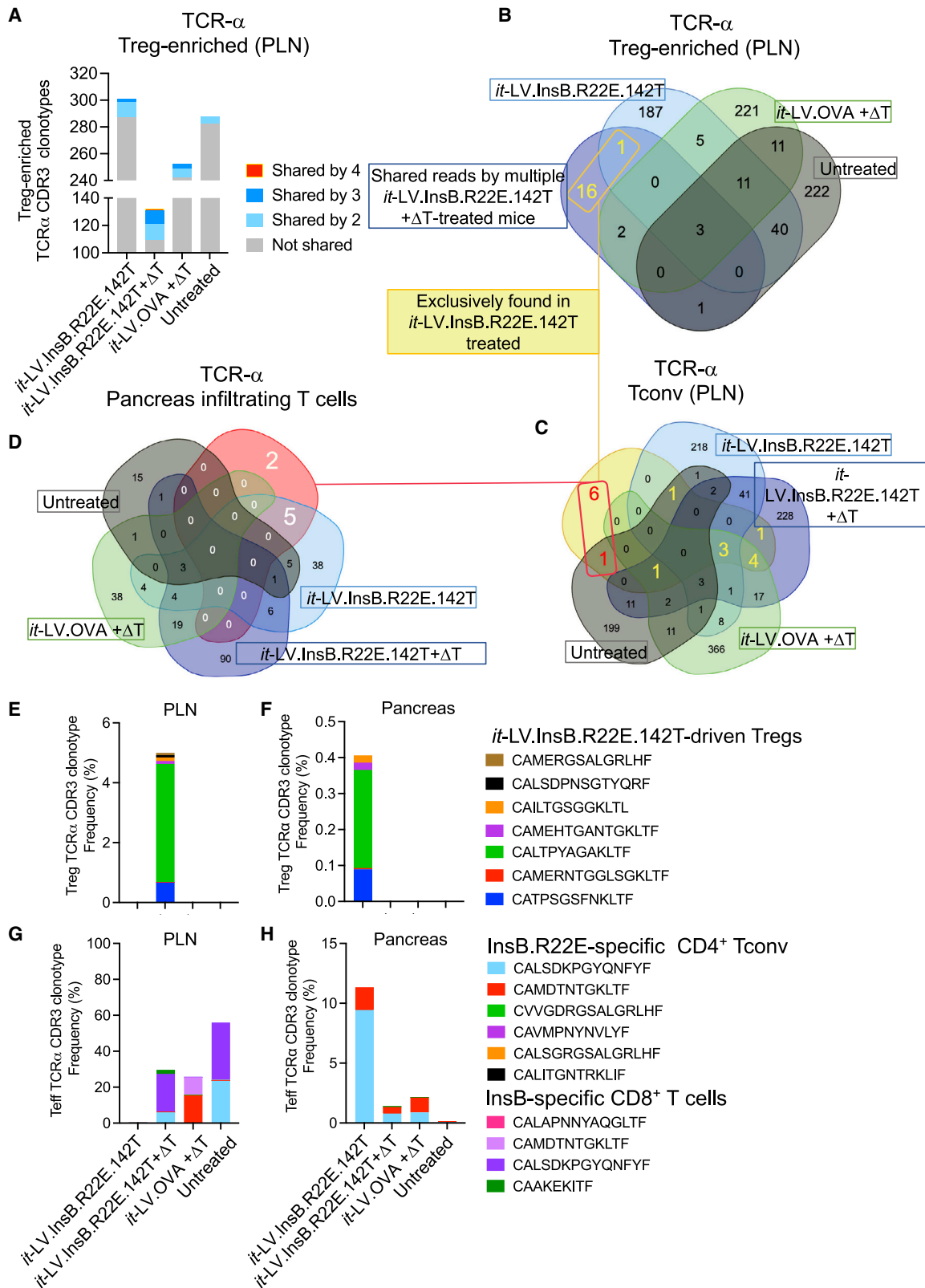
ease, as shown for InsB₉₋₂₃-specific T cells in NOD mice.²⁶ Furthermore, in recent studies conducted in humans genetically at risk for T1D, T cell responses to HIPs were more prevalent than responses to insulin peptides, and were strongly associated with formation of anti-insulin autoAbs and to T1D progression.^{25,27–29}

Micro-RNA142-regulated vector design avoids triggering of autoimmunity by activation of peripheral mature T cells and is mandatory for safety. Indeed, our study shows that a T cell-depleting regimen applied immediately after LV-mediated conditioning of thymus, although not effective *per se*, contributes to achieving a complete prevention of T1D, likely by removal of diabetogenic peripheral mature T cells at the time of treatment. However, we cannot exclude a role for thymic resident APCs in transgenic Ag

presentation, which may still be translated in the case of leakiness of micro-RNA142 regulation or acquired from thymic fibroblast.³⁰ Moreover, upon Ag-loaded-MHC class II exposure on the cell surface LV-modified TECs themselves may release an excess of transgenic Ag copies stored in the endosome, thus leading to a potential contribution in Ag presentation by professional APCs in the thymus.

Our results further highlight how strategies to temporarily deplete and inactivate peripheral T cells are insufficient in disarming diabetogenic T cell repertoire in NOD mice and in subjects at risk for T1D. Indeed, Herold et al. recently showed clinical results of a 14-day treatment with Teplizumab (anti-CD3 mAb) in a large cohort of genetically predisposed high-risk subjects. This T cell-directed regimen led to a significant delay of T1D onset, but it was unable to protect patients from disease progression.³¹ In this

thymocyte selection, we propose an innovative LV-mediated gene transfer approach specifically targeting TECs *in vivo* to generate presentation of MHC class I and II restricted epitopes, persisting beyond their typical 2-week turn-over time,¹⁹ as a consequence of TEC precursor transduction. AutoAg-derived epitopes may be modified to increase the strength of the TEC-thymocyte interaction, as for InsB₉₋₂₃R22E. This may be exploited to overcome the suboptimal selection of insulin-reactive clones by the wt-InsB₉₋₂₃ epitope and promote differentiation of insulin-specific Tregs. Moreover, our LV platform may potentially be applied to generate central tolerance to *neo*-Ags described both in humans with T1D and NOD mice (namely, hybrid insulin peptides [HIPs]), generated by post translational modification within secretory granules of β cells upon covalent binding of (pro)insulin peptides and other peptides derived from β cell-related Ags.²⁵ In murine models, HIP-specific T cells transfer dis-



(legend on next page)

context, strategies aimed at the correction of the central tolerance machinery may represent a concrete option for prevention of autoimmunity.

Expanding the clonality of insulin-specific Tregs by naturally occurring mechanisms may, in the long term, strengthen the regulatory arm of the immune system to regulate autoreactive cells spared by T cell-directed regimen. Although ethical concerns may arise from LV-based preventive treatment in pediatric at-risk subjects, our study suggests that an early intervention with intrathymic gene therapy associated with a T cell-depletion regimen may result in suppression of relevant autoimmune reaction prevalently occurring in lymphoid organs (PLN), as suggested by the localization of Treg clones in it-LV.InsB₉₋₂₃R22E.142T+ΔT-treated mice.

Discrepancies in maturation of T cell compartment and primary lymphoid organs in humans and mice have been considered. In humans, T cell compartment and lymphoid tissues are almost completely established at birth, and the thymus is fully active until puberty, when it starts to involute, turning into fatty tissue with residual activity of T cell selection. Conversely, mice are lymphopenic at birth with a small thymus that grows during the first weeks of life, while changes in the size and cortico-medullary structure become visible starting from 2.5 months. Involution of the thymus progressively evolves with age, preserving a basal activity to refill life-long naive T cell compartment.²⁰

Limitations of our strategy may derive from *in vivo* administration of integration-competent LV and from the choice of the autoAg. Several years of follow-up of patients enrolled in hematopoietic stem cell *ex vivo* gene therapy clinical trials^{32,33} did not show signs of genotoxicity in highly replicating cells, such as hematopoietic stem cells, with a pattern of integration in active genes, typical of the LV.³⁴ This also occurred in non-human primates undergoing LV *in vivo* gene transfer directed to hepatocytes.³⁵

Although T cell epitopes in T1D are well characterized based on the human HLA,³⁶ we envisage that a personalized it-LV therapy for T1D could be designed according to pre-screening T cell reactivity, with the possibility of including multiple target epitopes. Overall, our study may contribute to the definition of a strategy for prevention, not only for T1D, but generally applicable to T cell-mediated autoimmune diseases.

MATERIALS AND METHODS

Study design

To investigate whether the correction of T cell repertoire selection could abrogate susceptibility to T1D, NOD mice received an integration competent LV dose in the thymus to impose specific Ag presentation to developing thymocytes, followed by a T cell-depleting regimen. Mice were treated at the age of 5 weeks, largely before the onset of T1D but when insulin tolerance has already been broken *in vivo*. Experimental groups were dimensioned to allow statistical analysis. Mice were randomly assigned to each group, but the experimenter was not blinded to group identity.

Lentiviral vectors

InsulinB₄₋₂₉ (QHLCGSHLVEALYLVCGERGFFYTPM) and Insulin B₄₋₂₉R22E (QHLCGSHLVEALYLVCGEEGFFYTPM) or control Ovalbumin₃₁₅₋₃₅₃ (CGISSAESLKISQAVHAAHAEINEAGREVVGSAAEAGVDAAS) and GAD65₅₀₀₋₅₈₅ (HTNVCVFWFVPPSLRTLEDNEERMSRLSKVAPVIKARMMMEYGTMTMSYQPLGDKVNFRRMVISNPAATHQDIDFLIEEIERLGQDL) coding sequences were fused in-frame to murine invariant-chain (Ii),³⁷ including a Kozak sequence upstream of the transcription start site and a stop codon at the terminus. Therefore, sequences were cloned into linearized BamHI-SalI vectors for transgene expression: pCCLsin.PGK.wpre (LV.PGK), and pCCLsin.PGK.wpre142-3pT (LV.PGK.142T), including the ubiquitously active phosphoglycerate kinase promoter (PGK), and four repeated, microRNA142 target (142T) sequence.^{38,39} Third-generation LVs were produced by Ca₃PO₄ transfection into 293T cells and titrated as described previously.^{40,41}

Integrated vector quantification of copies

For mice experiments, DNA was extracted from thymus samples using Maxwell 16 Tissue DNA Purification Kit (Promega). VCN in murine DNA was determined by ddPCR, starting from 5–20 ng of template gDNA using a primers/probe set designed on the primer binding site region of LV, as described above for LV titration. The amount of endogenous murine DNA was quantified by a primers/probe set designed on the murine *sema3a* gene (Sema3A fw: 5'-ACCGATTCCAGATGATTGGC-3'; Sema3A rv: 5'-TCCATATTAATGCAGTGCTTGC-3'; Sema3A probe: HEX 5'-AGAGGCCTGTCC TGCAGCTCATGG-3' BHQ1).⁴² The PCR reaction was performed with each primer (900 nM) and the probe (250 nM) following the manufacturer's instructions (Bio-Rad), read with a QX200 reader

Figure 6. TCR α sequencing identified a family of Treg clones in PLN and pancreatic infiltration of mice, whose thymic selection has been conditioned by it-LV.InsB.R22E.142T

At the end of observation, a Treg-enriched population (CD4⁺CD25⁺CD127^{low/-}) was FACS sorted from it-treated NOD mice with LV.II.InsB₄₋₂₉.R22E.142T ± T cell depletion (it-LV.InsB.R22E.142T+ΔT, n = 7, it-LV.InsB.R22E.142T, n = 6), LV.OVA (n = 5) or untreated mice as control (n = 3). (A) TCR α sequencing was performed on sorted cells and sharing of CDR3 amino acid sequences was determined within multiple mice in each experimental group. Total number of TCR α chain clonotypes for each group is reported, highlighting those shared by multiple mice within each group. (B) Seventeen of the 23 TCR α amino acid sequences shared by Tregs of it-LV.InsB.R22E.142T+ΔT-treated NOD mice were selected to be associated to it-LV.InsB.R22E.142T treatment in PLN Treg-enriched. (C) Only seven of them are bona fide Tregs as they were not found in Tconv of PLN. (D) Five of the Treg-TCR α amino acid sequences were detectable in pancreatic infiltrates of it-LV.InsB.R22E.142T-treated NOD mice. (E and F) Frequencies of TCR α amino acid sequences in PLN and pancreas of bona fide Tregs associated to it-LV.InsB.R22E.142T-conditioned thymic selection are reported. (G and H) Similarly, frequencies in PLN and pancreas of TCR α amino acid sequences of InsB-specific T cells (CD8⁺ T cells and CD4⁺ Tconv) are reported.

and analyzed with QuantaSoft software (Bio-Rad). Transduced CEM (lymphoblastic cells line) clones carrying a known number of copies were used as standard and internal control. Results are expressed as VCN/diploid genome.

Mice and treatments

Female non-obese diabetic (NOD/LtJ), C57Bl6 (C57BL/6NCRl), C57Bl6 congenic CD45.1 (B6.SJL-*Ptprca*^a/*Pepc*^b/BoyCrl), and OT-II.C57Bl6 (C57BL/6-Tg(TcraTcrb)425Cbn/Crl) mice were purchased (Charles River, Calco, Italy) and housed in specific pathogen-free conditions. Diabetes was determined by two consecutive measures of glycemia ≥ 250 mg/dL. Blood glucose measurements were determined by a Bayer Breeze blood glucose monitoring system (Bayer). All procedures were reviewed and approved by the Institutional Animal Care and Use Committee at San Raffaele Institute, Milan (no. 1062).

Intrathymic LV injection in the thymus was performed as described previously.⁴³ In brief, mice were anesthetized and placed supine to make a small (4–5 mm) transverse incision of the skin in coincidence to a line joining the anterior legs to identify intercostal spaces. Two injections were performed by Hamilton syringe (Neuros, 33 gauge) through the second intercostal space on either side of the sternum with an $\sim 30^\circ$ – 40° angle to access both the thymic lobes. An LV dose of 2×10^7 TU/mouse was typically injected in a volume of 10–15 μ L/lobe. The skin was closed by stitches.

A mix containing anti-CD4 (100 μ g/dose, clone GK1.5) and anti-CD8 (100 μ g/dose, clone YTS169.4) depleting Abs (Bio X Cell) was administered intravenously. Transgene expression following it-LV.PGK.luciferase treatment was evaluated in NOD mice at the indicated time points by a small-animal bioluminescence imaging procedure using the IVIS Spectrum CT System (PerkinElmer).

OT-II chimeric mice conditioning and BM transplantation

BM from 6-week-old OT-II mice was harvested by flushing femurs. CD45.1 mice received total body irradiation (935 cGy split into two doses performed at least 2 h apart) protecting the thymus with a lead shield; afterward OT-II BM cells (7.5×10^6 cells/mouse) were injected intravenously. Mice were bled, and the engraftment of donor cells was determined by flow cytometry at weekly intervals.

Lymphocyte isolation and immunophenotyping

Spleens and PLNs were homogenized using frosted glass slides and filtered after RBC lyses (where needed) to obtain a single-cell suspension. Single-cell suspensions were stained with the following Abs: anti-CD4 (RM4-5), anti-CD8 (53–6.7) anti-CD62L (MEL14), anti-CD25 (PC61), anti-CD3 (17A2), anti-CD45 (30F11), anti-CD44 (IM7), anti-GR1 (RB6-8C5), anti-CD11b (M1/70), anti-CD45.1 (A20), anti-CD45.2 (104), anti-CD19 (1D3), anti-CD45RB/B220 (RA3-6B2), (BD Pharmingen), anti-CD11c (N418), and anti-Foxp3 (FjK-16s) (eBioscience). Intracellular Foxp3 staining was performed according to the manufacturer's instructions. Labeled cells were analyzed using a BD Symphony cytometer (BD) and analyzed using

Flowjo-10 software. Class II MHC tetramer IAg⁷ InsB₉₋₂₃R22E MHC class II (HLVERLYLVCGEEG) and MHC class I H2-K^d InsB₁₅₋₂₃ (LYLVCGERG) were provided by the NIH Tetramer Core (Emory University, Atlanta, GA).

TEC isolation and characterization

Murine TEC isolation was performed at the indicated time points following it-LV treatment. Murine thymus was cleaned of fat and stromal tissue, and then digested at 37°C with an enzymatic solution containing Liberase TL and DNase I. Digested tissues were collected in DMEM with 10% fetal bovine serum, 1% glutamine, and 1% penicillin and streptomycin. Single thymic cell suspensions were then incubated with anti-CD45 micro-beads (Miltenyi Biotec) and processed with the AutoMACS Pro Separator (Miltenyi Biotec). The CD45 negative fraction was retrieved and then tested by multiparametric cytofluorimetric analysis for the expression of TEC markers.⁴⁴

To check TEC enrichment after isolation, cells were immune-stained by anti-CD45 (clone 30-F11, BioLegend), anti-EpCAM (clone G8.8, BioLegend) and pan anti-major MHC class II (IA/IE MHC-II) (clone M5/114.15.2), anti-CD49F (GoH3) (BioLegend), anti-Ly5.1 (clone 6C3) (Miltenyi), and anti-CD80 (16-10A1) (BD Pharmingen). Exclusion of dead cells was done by adding 200 μ g/mL of DAPI solution just before acquisition.

Immunohistochemistry and islets scoring

Pancreata and thymi were harvested, fixed in 10% buffered formalin (Bio Optica) and embedded in paraffin. Serial sections (4 μ m) were stained with hematoxylin and eosin for morphological analysis and insulinitis scoring. To determine levels of insulinitis, we performed an unbiased software quantification analysis based on the Aperio Scan Software System. Thus, pancreatic islets were assigned as healthy islets with no lesions/infiltration: 1%–25%, 26%–50%, 51%–75%, and 76%–100% of infiltration/islet destruction.

To assess immunolocalization of Foxp3, rabbit anti-Foxp3 (FjK-16s) antibody was used after antigen retrieval with Tris-EDTA (pH 9) in a warm bath and revealed by rat on a rodent HRP-polymer and rabbit on a rodent HRP-polymer (Biocare Medical), using 3,3-diaminobenzidine as chromogen (BioGenex). Slides were counterstained with hematoxylin. To normalize Foxp3+Treg infiltration, the ratio between the area of Foxp3-stained and the area of infiltration of each single islet was measured using an unbiased software quantification analysis tool based on Aperio Scan Software System.

TCR α/β -sequencing

TCR α and β chains were sequenced using a modified rapid amplification of cDNA end PCR protocol, independent of multiplex PCR.⁴⁵ Total RNA extracted from FACS-sorted subpopulations was reverse transcribed and amplified using primers specific to murine α/β chain constant regions and for the template-switching sequence added during cDNA synthesis. PCR amplicons were purified with AMPure beads (Beckman Coulter) and sequenced on a MiSeq platform (Illumina). Data were analyzed using MiXCR software.⁴⁶ Non-functional

CDR3 amino acid sequences were excluded from the analysis using the VDJtools package.⁴⁷

Statistical analyses

Statistical analyses were performed using GraphPad Prism software. Incidence of diabetes was compared by Mantel-Cox test. Fisher's exact test (chi-square test) was used to compare levels of infiltration between experimental groups. ANOVA was used to determine statistical differences between multiple experimental groups, following verification of normal distribution of measurements in each group by Shapiro-Wilk test, while Mann-Whitney U test was used to compare means between two independent groups. Findings were considered significant with values for $p \leq 0.05$.

SUPPLEMENTAL INFORMATION

Supplemental information can be found online at <https://doi.org/10.1016/j.omtm.2022.04.017>.

ACKNOWLEDGMENTS

We thank R. Norata and V. Mauro for technical support in histological analyses (Tiget-GLP team); A. Nonis and F. and C. Di Serio for statistical consulting (CUSSEB); L. Passerini, F.R. Santoni De Sio, and all other members of the Mechanisms of Peripheral Tolerance Unit at SR-Tiget for helpful discussions. The graphical abstract was created with [BioRender.com](https://www.biorender.com). We thank the NIH Tetramer Core facility for provision of tetramers. This work was supported by the Italian Telethon Foundation (SR-Tiget core grant G2 2015-2020).

AUTHOR CONTRIBUTIONS

F.R., R.C., L.P., and I.B. designed and performed experiments and analyzed data. E.R. performed TCR sequencing. F.S. coordinated histological analyses. S.G. and A.V. interpreted data and edited the manuscript. A.A. designed and coordinated the project, interpreted data, and wrote the manuscript.

DECLARATION OF INTERESTS

The authors declare no competing interests.

REFERENCES

- Atkinson, M.A., Eisenbarth, G.S., and Michels, A.W. (2014). Type 1 diabetes. *Lancet* 383, 69–82. [https://doi.org/10.1016/s0140-6736\(13\)60591-7](https://doi.org/10.1016/s0140-6736(13)60591-7).
- Mayer-Davis, E.J., Lawrence, J.M., Dabelea, D., Divers, J., Isom, S., Dolan, L., Imperatore, G., Linder, B., Marcovina, S., Pettitt, D.J., et al. (2017). Incidence trends of type 1 and type 2 diabetes among youths, 2002–2012. *N. Engl. J. Med.* 376, 1419–1429. <https://doi.org/10.1056/nejmoa1610187>.
- Bot, A., Smith, D., Bot, S., Hughes, A., Wolfe, T., Wang, L., Woods, C., and von Herrath, M. (2001). Plasmid vaccination with insulin B chain prevents autoimmune diabetes in nonobese diabetic mice. *J. Immunol.* 167, 2950–2955. <https://doi.org/10.4049/jimmunol.167.5.2950>.
- Daniel, D., and Wegmann, D.R. (1996). Intranasal administration of insulin peptide B: 9–23 protects NOD mice from diabetes. *Ann. N.Y. Acad. Sci.* 778, 371–372. <https://doi.org/10.1111/j.1749-6632.1996.tb1146.x>.
- Fousteri, G., Dave, A., Bot, A., Juntti, T., Omid, S., and von Herrath, M. (2010). Subcutaneous insulin B:9–23/IFA immunisation induces Tregs that control late-stage prediabetes in NOD mice through IL-10 and IFN γ . *Diabetologia* 53, 1958–1970. <https://doi.org/10.1007/s00125-010-1777-x>.
- Roep, B.O., Solvason, N., Gottlieb, P.A., Abreu, J.R.F., Harrison, L.C., Eisenbarth, G.S., Yu, L., Leviten, M., Hagopian, W.A., Buse, J.B., et al. (2013). Plasmid-encoded proinsulin preserves C-peptide while specifically reducing proinsulin-specific CD8(+) T cells in type 1 diabetes. *Sci. Transl. Med.* 5, 191ra182. <https://doi.org/10.1126/scitranslmed.3006103>.
- Akbarpour, M., Goudy, K.S., Cantore, A., Russo, F., Sanvito, F., Naldini, L., Annoni, A., and Roncarolo, M.G. (2015). Insulin B chain 9–23 gene transfer to hepatocytes protects from type 1 diabetes by inducing Ag-specific FoxP3+ Tregs. *Sci. Transl. Med.* 7, 289ra281. <https://doi.org/10.1126/scitranslmed.aaa3032>.
- Russo, F., Citro, A., Squeri, G., Sanvito, F., Monti, P., Gregori, S., Roncarolo, M.G., and Annoni, A. (2021). InsB9–23 gene transfer to hepatocyte-based combined therapy abrogates recurrence of type 1 diabetes after islet transplantation. *Diabetes* 70, 171–181. <https://doi.org/10.2337/db19-1249>.
- Pugliese, A., Zeller, M., Fernandez, A., Jr., Zalcberg, L.J., Bartlett, R.J., Ricordi, C., Pietropaolo, M., Eisenbarth, G.S., Bennett, S.T., and Patel, D.D. (1997). The insulin gene is transcribed in the human thymus and transcription levels correlate with allelic variation at the INS VNTR-IDD2 susceptibility locus for type 1 diabetes. *Nat. Genet.* 15, 293–297. <https://doi.org/10.1038/ng0397-293>.
- Marodon, G., and Klatzmann, D. (2004). In situ transduction of stromal cells and thymocytes upon intrathymic injection of lentiviral vectors. *BMC Immunol.* 5, 18. <https://doi.org/10.1186/1471-2172-5-18>.
- Siatskas, C., Seach, N., Sun, G., Emerson-Webber, A., Silvain, A., Toh, B.H., Alderuccio, F., Backstrom, B.T., Boyd, R.L., and Bernard, C.C. (2012). Thymic gene transfer of myelin oligodendrocyte glycoprotein ameliorates the onset but not the progression of autoimmune demyelination. *Mol. Ther.* 20, 1349–1359. <https://doi.org/10.1038/mt.2012.15>.
- Nakayama, M., Abiru, N., Moriyama, H., Babaya, N., Liu, E., Miao, D., Yu, L., Wegmann, D.R., Hutton, J.C., Elliott, J.F., and Eisenbarth, G.S. (2005). Prime role for an insulin epitope in the development of type 1 diabetes in NOD mice. *Nature* 435, 220–223. <https://doi.org/10.1038/nature03523>.
- Thapa, P., and Farber, D.L. (2019). The role of the thymus in the immune response. *Thorac. Surg. Clin.* 29, 123–131. <https://doi.org/10.1016/j.thorsurg.2018.12.001>.
- Wong, K., Lister, N.L., Barsanti, M., Lim, J.M., Hammett, M.V., Khong, D.M., Siatskas, C., Gray, D.H., Boyd, R.L., and Chidgey, A.P. (2014). Multilineage potential and self-renewal define an epithelial progenitor cell population in the adult thymus. *Cell Rep.* 8, 1198–1209. <https://doi.org/10.1016/j.celrep.2014.07.029>.
- Brown, B.D., Venneri, M.A., Zingale, A., Sergi, L.S., and Naldini, L. (2006). Endogenous microRNA regulation suppresses transgene expression in hematopoietic lineages and enables stable gene transfer. *Nat. Med.* 12, 585–591. <https://doi.org/10.1038/nm1398>.
- Daniel, C., Weigmann, B., Bronson, R., and von Boehmer, H. (2011). Prevention of type 1 diabetes in mice by tolerogenic vaccination with a strong agonist insulin mimotope. *J. Exp. Med.* 208, 1501–1510. <https://doi.org/10.1084/jem.20110574>.
- Stadinski, B.D., Zhang, L., Crawford, F., Marrack, P., Eisenbarth, G.S., and Kappler, J.W. (2010). Diabetogenic T cells recognize insulin bound to IAg7 in an unexpected, weakly binding register. *Proc. Natl. Acad. Sci. U S A* 107, 10978–10983. <https://doi.org/10.1073/pnas.1006545107>.
- Crawford, F., Stadinski, B., Jin, N., Michels, A., Nakayama, M., Pratt, P., Marrack, P., Eisenbarth, G., and Kappler, J.W. (2011). Specificity and detection of insulin-reactive CD4+ T cells in type 1 diabetes in the nonobese diabetic (NOD) mouse. *Proc. Natl. Acad. Sci. U S A* 108, 16729–16734. <https://doi.org/10.1073/pnas.1113954108>.
- Gray, D.H.D., Seach, N., Ueno, T., Milton, M.K., Liston, A., Lew, A.M., Goodnow, C.C., and Boyd, R.L. (2006). Developmental kinetics, turnover, and stimulatory capacity of thymic epithelial cells. *Blood* 108, 3777–3785. <https://doi.org/10.1182/blood-2006-02-004531>.
- Manley, N.R., Richie, E.R., Blackburn, C.C., Condie, B.G., and Sage, J. (2011). Structure and function of the thymic microenvironment. *Front. Biosci.* 16, 2461–2477. <https://doi.org/10.2741/3866>.
- Simone, E., Daniel, D., Schloot, N., Gottlieb, P., Babu, S., Kawasaki, E., Wegmann, D., and Eisenbarth, G.S. (1997). T cell receptor restriction of diabetogenic autoimmune NOD T cells. *Proc. Natl. Acad. Sci. U S A* 94, 2518–2521. <https://doi.org/10.1073/pnas.94.6.2518>.

22. Marodon, G., Fisson, S., Levacher, B., Fabre, M., Salomon, B.L., and Klatzmann, D. (2006). Induction of antigen-specific tolerance by intrathymic injection of lentiviral vectors. *Blood* 108, 2972–2978. <https://doi.org/10.1182/blood-2006-03-010900>.
23. Lee, T., Sprouse, M.L., Banerjee, P., Bettini, M., and Bettini, M.L. (2017). Ectopic expression of self-antigen drives regulatory T cell development and not deletion of autoimmune T cells. *J. Immunol.* 199, 2270–2278. <https://doi.org/10.4049/jimmunol.1700207>.
24. Mohan, J.F., Petzold, S.J., and Unanue, E.R. (2011). Register shifting of an insulin peptide-MHC complex allows diabetogenic T cells to escape thymic deletion. *J. Exp. Med.* 208, 2375–2383. <https://doi.org/10.1084/jem.20111502>.
25. Delong, T., Wiles, T.A., Baker, R.L., Bradley, B., Barbour, G., Reisdorph, R., Armstrong, M., Powell, R.L., Reisdorph, N., Kumar, N., et al. (2016). Pathogenic CD4 T cells in type 1 diabetes recognize epitopes formed by peptide fusion. *Science* 351, 711–714. <https://doi.org/10.1126/science.aad2791>.
26. Wiles, T.A., Delong, T., Baker, R.L., Bradley, B., Barbour, G., Powell, R.L., Reisdorph, N., and Haskins, K. (2017). An insulin-IAPP hybrid peptide is an endogenous antigen for CD4 T cells in the non-obese diabetic mouse. *J. Autoimmun.* 78, 11–18. <https://doi.org/10.1016/j.jaut.2016.10.007>.
27. Mannering, S.I., Harrison, L.C., Williamson, N.A., Morris, J.S., Thearle, D.J., Jensen, K.P., Kay, T.W., Rossjohn, J., Falk, B.A., Nepom, G.T., and Purcell, A.W. (2005). The insulin A-chain epitope recognized by human T cells is posttranslationally modified. *J. Exp. Med.* 202, 1191–1197. <https://doi.org/10.1084/jem.20051251>.
28. Baker, R.L., Rihanek, M., Hohenstein, A.C., Nakayama, M., Michels, A., Gottlieb, P.A., Haskins, K., and Delong, T. (2019). Hybrid insulin peptides are autoantigens in type 1 diabetes. *Diabetes* 68, 1830–1840. <https://doi.org/10.2337/db19-0128>.
29. Mitchell, A.M., Alkanani, A.A., McDaniel, K.A., Pyle, L., Waugh, K., Steck, A.K., Nakayama, M., Yu, L., Gottlieb, P.A., Rewers, M.J., and Michels, A.W. (2021). T-cell responses to hybrid insulin peptides prior to type 1 diabetes development. *Proc. Natl. Acad. Sci. U S A* 118. e2019129118.
30. Nitta, T., Tsutsumi, M., Nitta, S., Muro, R., Suzuki, E.C., Nakano, K., Tomofuji, Y., Sawa, S., Okamura, T., Penninger, J.M., and Takayanagi, H. (2020). Fibroblasts as a source of self-antigens for central immune tolerance. *Nat. Immunol.* 21, 1172–1180. <https://doi.org/10.1038/s41590-020-0756-8>.
31. Herold, K.C., Bundy, B.N., and Krischer, J.P.; Type 1 Diabetes TrialNet Study Group (2019). Teplizumab in relatives at risk for type 1 diabetes. Reply. *N. Engl. J. Med.* 381, 1880–1881. <https://doi.org/10.1056/NEJMc1912500>.
32. Aiuti, A., Biasco, L., Scaramuzza, S., Ferrua, F., Cicalese, M.P., Baricordi, C., Dionisio, F., Calabria, A., Giannelli, S., Castiello, M.C., et al. (2013). Lentiviral hematopoietic stem cell gene therapy in patients with Wiskott-Aldrich syndrome. *Science* 341, 1233151. <https://doi.org/10.1126/science.1233151>.
33. Sessa, M., Lorioli, L., Fumagalli, F., Acquati, S., Redaelli, D., Baldoli, C., Canale, S., Lopez, I.D., Morena, F., Calabria, A., et al. (2016). Lentiviral haemopoietic stem-cell gene therapy in early-onset metachromatic leukodystrophy: an ad-hoc analysis of a non-randomised, open-label, phase 1/2 trial. *Lancet* 388, 476–487. [https://doi.org/10.1016/s0140-6736\(16\)30374-9](https://doi.org/10.1016/s0140-6736(16)30374-9).
34. Cesana, D., Ranzani, M., Volpin, M., Bartholomae, C., Duros, C., Artus, A., Merella, S., Benedicenti, F., Sergi, L., Sanvito, F., et al. (2014). Uncovering and dissecting the genotoxicity of self-inactivating lentiviral vectors in vivo. *Mol. Ther.* 22, 774–785. <https://doi.org/10.1038/mt.2014.3>.
35. Milani, M., Annoni, A., Moalli, F., Liu, T., Cesana, D., Calabria, A., Bartolaccini, S., Biffi, M., Russo, F., Visigalli, I., et al. (2019). Phagocytosis-shielded lentiviral vectors improve liver gene therapy in nonhuman primates. *Sci. Transl. Med.* 11, eaav7325. <https://doi.org/10.1126/scitranslmed.aav7325>.
36. Di Lorenzo, T.P., Peakman, M., and Roep, B.O. (2007). Translational mini-review series on type 1 diabetes: systematic analysis of T cell epitopes in autoimmune diabetes. *Clin. Exp. Immunol.* 148, 1–16. <https://doi.org/10.1111/j.1365-2249.2006.03244.x>.
37. Arce, F., Rowe, H.M., Chain, B., Lopes, L., and Collins, M.K. (2009). Lentiviral vectors transduce proliferating dendritic cell precursors leading to persistent antigen presentation and immunization. *Mol. Ther.* 17, 1643–1650. <https://doi.org/10.1038/mt.2009.149>.
38. Annoni, A., Brown, B.D., Cantore, A., Sergi, L.S., Naldini, L., and Roncarolo, M.G. (2009). In vivo delivery of a microRNA-regulated transgene induces antigen-specific regulatory T cells and promotes immunologic tolerance. *Blood* 114, 5152–5161. <https://doi.org/10.1182/blood-2009-04-214569>.
39. Brown, B.D., Cantore, A., Annoni, A., Sergi, L.S., Lombardo, A., Della Valle, P., D'Angelo, A., and Naldini, L. (2007). A microRNA-regulated lentiviral vector mediates stable correction of hemophilia B mice. *Blood* 110, 4144–4152. <https://doi.org/10.1182/blood-2007-03-078493>.
40. Follenzi, A., and Naldini, L. (2002). HIV-based vectors. Preparation and use. *Methods Mol. Med.* 69, 259–274. <https://doi.org/10.1385/1-59259-141-8:259>.
41. Annoni, A., Cantore, A., Della Valle, P., Goudy, K., Akbarpour, M., Russo, F., Bartolaccini, S., D'Angelo, A., Roncarolo, M.G., and Naldini, L. (2013). Liver gene therapy by lentiviral vectors reverses anti-factor IX pre-existing immunity in haemophilic mice. *EMBO Mol. Med.* 5, 1684–1697. <https://doi.org/10.1002/emmm.201302857>.
42. Matrai, J., Cantore, A., Bartholomae, C.C., Annoni, A., Wang, W., Acosta-Sanchez, A., Samara-Kuko, E., De Waele, L., Ma, L., Genovese, P., et al. (2011). Hepatocyte-targeted expression by integrase-defective lentiviral vectors induces antigen-specific tolerance in mice with low genotoxic risk. *Hepatology* 53, 1696–1707. <https://doi.org/10.1002/hep.24230>.
43. de la Cueva, T., Naranjo, A., de la Cueva, E., and Rubio, D. (2007). Refinement of intrathymic injection in mice. *Lab Anim. (NY)* 36, 27–32. <https://doi.org/10.1038/labani0507-27>.
44. Bortolomai, I., Sandri, M., Draghici, E., Fontana, E., Campodoni, E., Marcovecchio, G.E., Ferrua, F., Perani, L., Spinelli, A., Canu, T., et al. (2019). Gene modification and three-dimensional scaffolds as novel tools to allow the use of postnatal thymic epithelial cells for thymus regeneration approaches. *Stem Cell Transl. Med.* 8, 1107–1122. <https://doi.org/10.1002/sctm.18-0218>.
45. Bolotin, D.A., Mamedov, I.Z., Britanova, O.V., Zvyagin, I.V., Shagin, D., Ustyugova, S.V., Turchaninova, M.A., Lukyanov, S., Lebedev, Y.B., and Chudakov, D.M. (2012). Next generation sequencing for TCR repertoire profiling: platform-specific features and correction algorithms. *Eur. J. Immunol.* 42, 3073–3083. <https://doi.org/10.1002/eji.201242517>.
46. Bolotin, D.A., Poslavsky, S., Mitrophanov, I., Shugay, M., Mamedov, I.Z., Putintseva, E.V., and Chudakov, D.M. (2015). MiXCR: software for comprehensive adaptive immunity profiling. *Nat. Methods* 12, 380–381. <https://doi.org/10.1038/nmeth.3364>.
47. Shugay, M., Bagaev, D.V., Turchaninova, M.A., Bolotin, D.A., Britanova, O.V., Putintseva, E.V., Pogorelyy, M.V., Nazarov, V.I., Zvyagin, I.V., Kirgizova, V.I., et al. (2015). VDJtools: unifying post-analysis of T cell receptor repertoires. *PLoS Comput. Biol.* 11, e1004503. <https://doi.org/10.1371/journal.pcbi.1004503>.